

Surrogate model of the thermoforming of fiber reinforced thermoplastics

MIDDELHOFF Jan^{1,a*}, UJVARI Csenger^{1,b}, HÜRKAMP André^{1,c}
and DRÖDER Klaus^{1,d}

¹Technische Universität Braunschweig, Institute of Machine Tools and Production Technology,
Langer Kamp 19b, 38106 Braunschweig, Germany

^aj.middelhoff@tu-braunschweig.de, ^bujvari@tu-braunschweig.de,
^ca.huerkamp@tu-braunschweig.de, ^dk.droeder@tu-braunschweig.de

Keywords: Thermoforming, Composite Forming, Machine Learning, Artificial Neural Networks, Surrogate Modelling

Abstract. In the thermoforming process shearing of fiber reinforced thermoplastics (FRTP) leads to wrinkle formation and is therefore one of the most critical deformation mechanism. The target value to predict wrinkle formation is the shear angle which is considered in this paper. To predict the shear angle distribution during the thermoforming of FRTPs a Convolutional Neural Network (CNN) is used. The approach is based on the consideration of the principal curvature characteristics, resulting in the reduction of any complex geometry to planar, parabolic, elliptical, semi-spherical and hyperbolic areas. In similar research, CNNs are trained for each specific geometry. In this work, the CNN refers to a database of the mentioned curvature characteristics. In theory, all forming geometries can be created from these, which is why the CNN is enabled to predict the forming result of any complex geometry. In this paper, the benchmark geometry of a double dome is selected as the validation geometry and the error in the prediction of the shear angle is compared with the results of numerical forming simulations performed.

Introduction

Due to their high mechanical properties combined with low densities, FRTPs offer a high potential for lightweight design applications. The production of flat components made of FRTP is often realised by the thermoforming process, which represents a high potential for large-scale production [1]. Thermoforming usually involves heating fiber reinforced thermoplastic sheets (organo sheets) above the melting temperature of the matrix to enable draping of the fibers in the melt-viscous matrix during the forming process.

The draping behaviour is mainly determined by the in-plane shear property of the organo sheet. Furthermore, the different deformation modes transverse compression, out-of-plane bending and in-plane tension are important variables which influence the formability of the material and thus the forming result [2]. Accordingly, multiple defects such as wrinkling or fiber fracture can occur due to excessive shear stresses or tensile stresses [2]. The defects are mainly reduced by the selection of suitable process parameters, which increases the component quality. In addition to adjusted process parameters, additional technical supporting structures such as clamping systems or blank holders can be used to reduce the formation of wrinkles through the application of in-plane tensile stresses [3]. Due to the different influences of process parameters and additional supporting structures on the occurrence of defects, large cavity depths, sharp geometric transitions and three-dimensional space corners are difficult to produce and object complexity is limited [4]. A possible process adjustment for an increase in part quality for complex cavities is the implementation of stepwise forming with segmented stamps [5]. Due to this innovative tool concept, the parameter space of the process is increased. However, in order to avoid inefficient and expensive experiments, numerical investigations were implemented in order to examine

optimal segmentation and sequencing strategies for selected cavities. The numerical modelling of FRTPs even on the most common used macro-scale is timesensitive due to the complex material behaviour, thus surrogate models are useful for further time savings in the prediction of suitable segmentation and sequencing strategies. These types of Machine Learning (ML) architectures are already able to model the forming behaviour of different geometries as well as different process conditions [6]. These approaches will be addressed in this paper and extended with the approach explained in the following chapter. The presented investigations are the basis for further work on the implementation of the ML-based prediction of segmentation and sequencing strategies for increasing the prediction quality of shear stresses.

Curvature Analysis Approach

The goal of this research is to link a shear angle as the target variable with curvature values derived from the geometry of the cavity. The implementation of different basic geometries as a database enables a deep learning architecture the prediction of shear angles for all possible geometries.

The target value is the shear angle, which represents an important parameter for the prediction of local wrinkling, while the input value is given by the curvature of an examined complex cavity. This approach was derived from Coutadin et al. and developed further [7]. In this previous research, an existing tool geometry is imported as an STL file and the curvatures of the cavity are calculated. In the areas that exceed a previously defined critical curvature value, a segmentation cut is applied. Sequencing is further performed through a genetic optimisation algorithm. In the work of Zimmerling et al. [8], the topology of the test geometry is imported into the convolutional neural network as greyscale images as well as the output of the shear angle. The approach presented in this paper differs from [7] by reducing the data set for the CNN to the 5 most frequently occurring curvature characteristics. This avoids the necessity of a continuous implementation of new test geometries, since the description of all forms of complex geometries is possible using the five main forms of curvature. The methodology behind the approach is illustrated in Fig. 1.

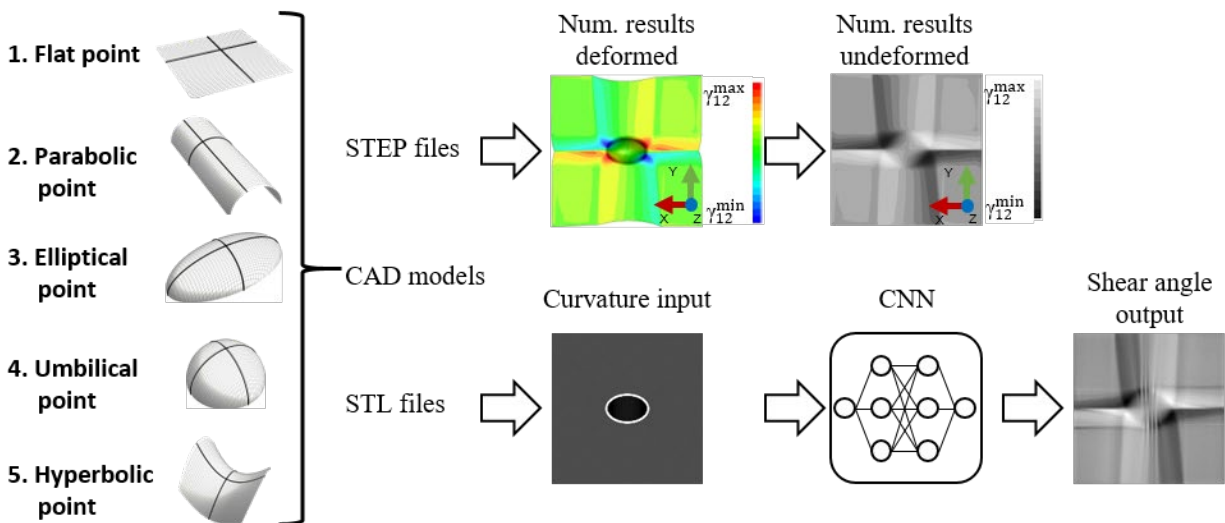


Fig. 1. Workflow of the curvature analysis approach.

The five relevant curvature characteristics are shown on the left. Out of these, the first four curvatures shown in Fig. 1 are considered in this paper. All curvatures are dependent on the two principal curvature components κ_1 and κ_2 . If $\kappa_1 = \kappa_2 = 0$, a flat point results. Accordingly, a planar surface is defined by this point. A parabolic point exists if the product of the two curvatures is $\kappa_1 \cdot \kappa_2 = 0$, with $\kappa_1 + \kappa_2 \neq 0$. An elliptical point is defined by $\kappa_1 \cdot \kappa_2 > 0$. A special type of the elliptic point exists for $\kappa_1 = \kappa_2$. This is referred to as the umbilical point, which results in a hemispherical geometry. The case of a hyperbolic point, considered in further work, occurs if $\kappa_1 \cdot \kappa_2 < 0$. [9]

Parameterized CAD models were developed from the curvature components illustrated and a large number of geometry variants were created. From these, STL files were derived, which are used for the curvature calculation. In this work, the mean curvature H (see Eq. 1) is applied, which represents the arithmetic mean of the two principal curvatures.

$$H := \frac{1}{2}(\kappa_1 + \kappa_2) \quad (1)$$

Numerical models are built for the individual surface curvatures in order to create an FEM database for the surrogate model. The models represent the pure curvature types, therefore no boundary effects occur in the output of the shear angle. Therefore, the resulting shearing effects exclusively result from the curvature types.

The calculated curvature values are then combined with results on the shear angle of the simulations. As a result, the curvature values are assigned with the shear angle distribution for the material used and provides the surrogate model with a training data set. The coupling enables the surrogate model to predict complex geometries not previously trained, since the local geometric characteristics of the cavity can be reduced to the previously trained curvature characteristics.

Parametrization

For the creation of the CAD models, the parameterization of the ellipse and the paraboloid visualized in Fig. 2 is chosen. The outer dimensions of the die, which also equal the main dimensions of the organosheet, were left constant. For the ellipse, variants were created in the intervals shown for the radii R_{ye} and R_{xe} with a step size of 1 mm for the database. With the same step size, variants with variable radius R_{xp} and variable depth were created for the models of the paraboloid. For the visualisation of the occurring curvature characteristics of the geometries as well as for the representation of the simulation results in the undeformed sheet, greyscale images are used based on Zimmerling et al. [8]. The geometry variants created are further transferred as a step file to the automated numerical model generation in the software LS-Dyna.

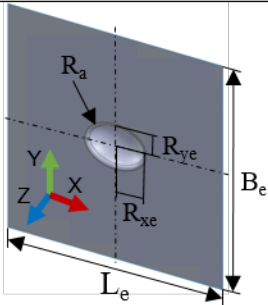
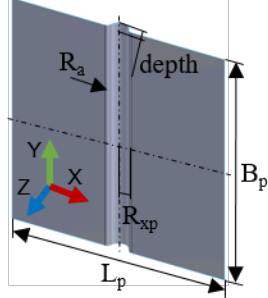
Ellipse	Symbol	Parameter	Interval
	L_e	Length die ellipse	235 mm
	B_e	Width die ellipse	235 mm
	R_{ye}	Radius y-direction ellipse	20...50 mm
	R_{xe}	Radius x-direction ellipse	30...60 mm
	R_a	Outer Radius	4 mm
Paraboloid	Symbol	Parameter	Interval
	L_p	Length die paraboloid	235 mm
	B_p	Width die paraboloid	235 mm
	R_{xp}	Radius x-direction paraboloid	10...50 mm
	R_a	Outer Radius	4 mm
	depth	Depth paraboloid	10...60 mm

Fig. 2. Parametrisation of elliptical and parabolic models with the parameter-range for generation of the training dataset.

Numerical Model

In the FEM software tool LS-Dyna, an isothermal forming simulation is set up consisting of punch, die and sheet. The blank is a glass fiber reinforced organo sheet with polyamide 6 matrix (Tepex dynalite 102RG600(4)/47%). The fabric is an E-Glass roved in twill 2/2 style with 47% fiber content and a total thickness of 2 mm. In the forming simulation, the temperature is chosen marginally above the matrix melting temperature, which is around 220°C for polyamide 6. Punch and die are modelled as rigid bodies, while the organo sheet is described by the material card MAT_249_REINFORCED_THERMOPLASTIC [10]. Within this material card, the fibers are described as an anisotropic-hyperelastic material and the matrix as elasto-plastic. The material card has been calibrated and validated in previous work using tensile and bias extension tests. A disadvantage of the material card is the lack of options for implementing bending stiffnesses. For numerical models using shell elements, the stiffness is unrealistically high, due to the fact that in classical approaches such as the Kirchhoff theory, the bending stiffness is given by the tensile stiffness and thickness while slippage between fibers leading to lower bending stiffness is not considered [11]. Therefore, the bending behaviour is adjusted through the position and number of integration points to the neutral axis of the sheet [12]. The friction between the individual contact pairs was investigated using a friction test setup. From these investigations, values for the friction coefficients above the matrix melting temperature at 230°C are obtained and used.

As a result of the simulation, the shear angle is given, which is projected onto the mesh of the initial sheet. Therefore the element-size was set to 2 mm, resulting in a mesh with 117x117 elements. This is exported together with the element IDs and the coordinates of the nodal points in order to couple the shear angles with the curvatures of the cavity in the subsequent step.

Design of the Artificial Neural Network

In this research, CNNs, which are a kind of feed-forward network, are used because they are specially designed for spatially structured data such as the grey-scale mesh resulting from the previous chapter [8]. The basic structure of a CNN consists of an input, several convolutional and pooling layers and the output. The activity of each neuron is determined by stepwise comparison with smaller convolutional matrices (kernels) moved over the input. In the process, each kernel extracts different features from the input data, allowing the individual activated neurons of deeper layers to abstract only local sections of the entire input data and creating what is called a "feature map". In deeper layers, the data is further compressed, which enables the detection of more complex features. Subsequently, compressed data is decoded in the decoder by transposed convolutional layers. [13]

The CNN presented in this paper is built using the deep learning framework PyTorch and the library fastai. A total of 87 variants of ellipses, 31 paraboloids and 10 planar surfaces were taken as the dataset, which was split randomly into 90% training data and 10% validation data. The training data set was divided into 16 batches and a total of 300 epochs were trained. First, the elliptical variants were trained for 200 epochs, followed by the parabolic and planar surface variants. The batch normalisation implemented in PyTorch counteracts an internal covariate shift and ensures a high learning rate in the network [14]. In a subsequent step, we tested variants of each geometry with out-of test range parameters and two previously unseen double-dome geometries with the CNN in order to investigate the prediction quality of this curvature approach.

Results and Discussion

Fig. 3 shows the results of the training geometries of a flat surface (plate), the parabolic and the elliptical geometries. In addition to the listed geometries, the curvatures serving as input for the CNN and the results of the FEM simulations are presented as comparative images. The simulation results are visualised on the undeformed blank and display the shear angle distribution as a greyscale image. The representation of the curvatures and the FEM simulations each represent normalised values within fixed limits to ensure comparability. Furthermore, three result values of the prediction are shown. The root mean square error (RMSE) along with the minimum and maximum shear angle differences $|\Delta\gamma_{12}^{min}|$ and $|\Delta\gamma_{12}^{max}|$ of the prediction compared to the FEM results. The shear angle differences are calculated by subtracting the shear angle obtained from the numerical model from the predicted shear angle.




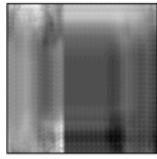
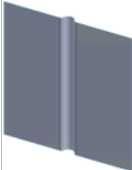


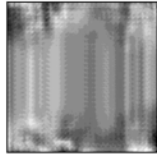


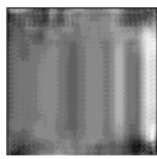
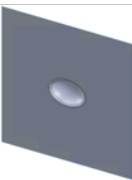
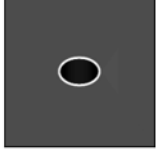
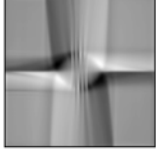


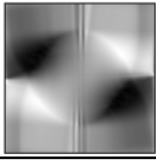
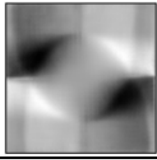
Geometry	Curvature	FEM-Result	CNN Prediction	RSME	$ \Delta\gamma_{12}^{min} $	$ \Delta\gamma_{12}^{max} $
				2.48°	3.39°	3.09°
				0.78°	1.27°	1.36°
				0.98°	1.15°	1.82°
				2.40°	1.38°	0.28°
				3.81°	0.02°	1.96°

Fig. 3. Visualisation of the test geometries, their curvatures and the results for the shear angle from the FEM-Model and from the CNN Prediction.

For ellipse and paraboloid, the smallest (top) and the largest (bottom) parameter combination are shown, which were examined during testing, but not part of the training data. The comparison of the result images and values shows a high agreement between simulation and prediction of the CNN. Here, the percentage error values for the plate are 4.33 %, while the error for the parabolic validation geometries is below 2 %. The error of the ellipse can also be described as low with 4.19 % for the smallest parameter combination (top image ellipse in Fig. 3) and 6.65 % for the largest combination, so that a reliable prediction of the shear angle can be achieved through the curvature images with a very small data set.

As a final validation, a complex geometry of a double dome, which was not part of any previously used dataset, was examined with the CNN. Two configurations were chosen as examples, which are visualised in Fig. 4. The double dome is composed of the two trained curvature variants of the ellipse and the paraboloid. The network was presented with both a double dome with identical ellipses (bottom) and a double dome with elliptical areas of different sizes (top).


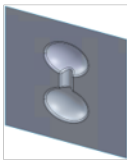
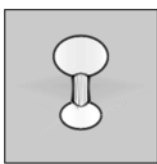


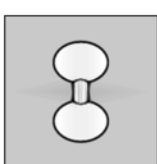


Geometry	Curvature	FEM-Result	CNN Prediction	RSME	$ \Delta\gamma_{12}^{min} $	$ \Delta\gamma_{12}^{max} $
 				13.61°	9.32°	10.79°
				16.23°	10.54°	12.87°

Fig. 4. Visualisation of Double-Dome Geometry, its curvatures and the results for the shear angle from the FEM-Model and from the CNN Prediction.

As shown in the result values, the RSME of the double-dome geometry with elliptical areas of different sizes is lower than the RSME of the double-dome geometry with two ellipses of the same size. Nevertheless, both errors are larger than the test errors of the elliptical, parabolic and planar geometries, with a percentage deviation of over 20 %. This is particularly visible in the transition between the elliptical and parabolic sub-area, which is not reliably predicted by the CNN. One reason for this may be the hyperbolic course in the transition, so that in further work the fifth curvature variant of hyperbolic geometries should be implemented for a more accurate result.

Summary

In the thermoforming process for manufacturing flat components from thermoplastic fiber composites, one of the main deformation mechanisms is shear deformation. As a result of high shear angles in the composite, wrinkles occur during the forming process. Predicting the shear angle as a parameter for localisation of upcoming wrinkles is therefore of central importance, hence the reliable prediction of this parameter was carried out in this paper by means of a Convolutional Neural Network. The results of numerical forming simulations provided the basis for the data. The training of the network was done by using only the occurring curvatures to predict the forming result of unseen, complex geometries (double dome) on the basis of the shear angle with a currently increased error in the range of 23 % to 28 %. In further work, the remaining curvature of a hyperbolic structure will be added to the database and further adjustments to the CNN will be applied. This should ensure in future that the neural network can reduce all complex geometries to the 5 curvature characteristics and thus provide a reliable prediction with a lower error for the selected target variable.

Acknowledgements

The IGF-Project “Material-specific thermoforming through controlled mould elements” of the European Research Association for Sheet Metal Working (EFB e.V.) was funded by the Federal Ministry of Economics and Energy (BMW i) under the funding number 20677BG of the German Federation of Industrial Research Associations (AiF) on the basis of a decision by the German Bundestag. The authors are thankful for this financial support.

References

- [1] C. Hopmann, M. Walter, Einführung in die Kunststoffverarbeitung, Carl Hanser Verlag GmbH & Co. KG, 2015.
- [2] R. Azzouz, S. Allaoui, R. Moulart, Composite preforming defects: a review and a classification, Int. J. Mater. Form. 14 (2021) 1259-1278. <https://doi.org/10.1007/s12289-021-01643-7>

- [3] U. Breuer, M. Neitzel, V. Ketzer, R. Reinicke, Deep drawing of fabric-reinforced thermoplastics: Wrinkle formation and their reduction, *Polym. Compos.* 17 (1996) 643-647. <https://doi.org/10.1002/pc.10655>
- [4] K. Dröder, *Prozesstechnologie zur Herstellung von FVK-Metall-Hybriden*, Springer Berlin Heidelberg, Berlin, Heidelberg, 2020.
- [5] J. Middelhoff, A. Hürkamp, K. Dröder, Numerical Modelling of a Demonstrator to Investigate Geometric Parameter Influences on the Thermoforming of Fiber-Reinforced Thermoplastics, *Proceedings of the 20th European Conference on Composite Materials, ECCM20, Lausanne, Switzerland, 2022*
- [6] C. Zimmerling, D. Dörr, F. Henning, L. Karger, A meta-model based approach for rapid formability estimation of continuous fibre reinforced components, *AIP Conference Proceedings, Volume 1960(1), 2018*, pp. 020042. <https://doi.org/10.1063/1.5034843>
- [7] S. Coutandin, *Prozessstrategien für das automatisierte Preforming von bebinderten textilen Halbzeugen mit einem segmentierten Werkzeugsystem*, Dissertation, Shaker Verlag
- [8] C. Zimmerling, D. Trippe, B. Fengler, L. Karger, An approach for rapid prediction of textile draping results for variable composite component geometries using deep neural networks. In: *Proceedings of the 22nd International ESAFORM Conference on Material Forming: ESAFORM 2019*, AIP Publishing, 2019, pp. 20007 <https://doi.org/10.1063/1.5112512>
- [9] W. Kühnel, *Differentialgeometrie: Kurven - Flächen - Mannigfaltigkeiten, 5., aktualisierte Auflage*, Springer eBook Collection. Vieweg+Teubner, Wiesbaden, 2010
- [10] A. Hürkamp, R. Lorenz, T. Ossowski, B.-A. Behrens, K. Dröder, Simulation-based digital twin for the manufacturing of thermoplastic composites, *Procedia CIRP* 100 (2021) 1-6. <https://doi.org/10.1016/j.procir.2021.05.001>
- [11] P. Boisse, R. Akkerman, P. Carlone, L. Kärger, S.L. Lomov, J.A. Sherwood, Advances in composite forming through 25 years of ESAFORM, *Int. J. Mater. Form.* 15 (2022). <https://doi.org/10.1007/s12289-022-01682-8>
- [12] M. Grubenmann, J. Heingärtner, P. Hora, D. Bassan, Influence of temperature on in-plane and out-of-plane mechanical behaviour of GFRP composite. *J. Phys.: Conf. Ser.* 1063 (2018) 12146. <https://doi.org/10.1088/1742-6596/1063/1/012146>
- [13] S. Kollmannsberger, D. D'Angella, M. Jokeit, L. Hermann, *Deep Learning in Computational Mechanics: An Introductory Course (Studies in Computational Intelligence, 977)*, Springer International Publishing, Cham, 2021
- [14] S. Ioffe, C. Szegedy, Batch Normalization: Accelerating Deep Network Training by Reducing Internal Covariate Shift, In: *International Conference on machine learning, 2015* pp. 448-456. <https://doi.org/10.48550/arXiv.1502.03167>